



Synthesis and Spectral Characterization of 14- and 16-membered tetraazamacrocyclic Schiff base ligands and their transition metal complexes and a comparative study of interaction of calf thymus DNA with copper(II) complexes

Tahir Ali Khan^{a,*}, Sultana Naseem^a, Shahper N. Khan^b, Asad U. Khan^b, Mohammad Shakir^{a,1}

^a Division of Inorganic Chemistry, Department of Chemistry, Aligarh Muslim University, Aligarh-202002, India

^b Interdisciplinary Biotechnology Unit, Aligarh Muslim University, Aligarh-202002, India

ARTICLE INFO

Article history:

Received 25 September 2008

Received in revised form 28 February 2009

Accepted 16 March 2009

Keywords:

Schiff base macrocyclic ligands

Spectral studies

Square planar complexes

Octahedral complexes

DNA binding studies

ABSTRACT

14 and 16 membered Schiff base macrocyclic ligands, 7,14-dimethyl-5,12-di(N-amino)-2-methylphenyl-1,4,8,11-tetraaza-cyclotetradecane-4,7,11,14-tetraene (L^1) and 8,16-dimethyl-6,14-di(N-amino)-2-methylphenyl-1,5,9,13-tetraaza-cyclohexadecane-5,8,13,16-tetraene (L^2) were synthesized by condensation reaction between 2'-methylacetoacetanilide and aliphatic diamines. The metal complexes of the types, $[ML^1](NO_3)_2$ and $[ML^2](NO_3)_2$ [$M = Co(II), Ni(II), Cu(II)$ and $Zn(II)$] were prepared by interaction of ligands, L^1 or L^2 with hydrated metal(II) nitrates. The ligands and their complexes were characterized by elemental analysis, IR, 1H and ^{13}C NMR, EPR, UV–Vis spectroscopy, magnetic susceptibility, conductivity measurements and ESI-mass spectral studies. The results of elemental analyses, ESI-mass and conductivity measurements confirmed the stoichiometry of ligands and their complexes while the characteristic absorption bands and resonance peaks in IR and NMR spectra confirmed the formation of ligand frameworks around the metal ions. The square planar geometry for complexes derived from ligand L^1 and octahedral environment for complexes derived from ligand L^2 with distortion in $Cu(II)$ complex have been confirmed on the basis of results of electronic and electron spin resonance spectral studies and magnetic moment measurements. Absorption and fluorescence spectral studies revealed different binding mode for complex, $[CuL^1](NO_3)_2$ as compared with $[CuL^2](NO_3)_2$ on interaction with calf thymus DNA.

© 2009 Elsevier B.V. All rights reserved.

1. Introduction

Schiff base macrocycles were among the first artificial metal macrocyclic complexes to be synthesized [1]. Studies on complexes of Schiff base macrocyclic ligands have received considerable attention in view of their applications [2–6] development of coordination and bioinorganic chemistry [7,8] models for biologically occurring metalloenzymes [9,10] and biomedical significance [11]. A large variety of [1 + 1] and [2 + 2] macrocyclic ligands have been reported defining the role of donor atoms, their relative positions, the number and size of the chelating rings, the flexibility and the shapes of the coordinating moiety on the selective binding of charged or neutral species and the properties arising from these aggregations [12,13]. Recognition of the importance of com-

plexes containing macrocyclic ligands for supramolecular science, bioinorganic chemistry, biomedical applications, separation and encapsulation processes as well as formation of compounds with unusual properties and structures tempted the chemists all over world to develop methods for the synthesis of these compounds. Many rational synthetic routes to macrocyclic ligands involve the use of a metal ion as template to orient the reacting groups to linear substrates in the desired conformation prior to ring closure [1,14]. The Schiff base have also been employed as ligands for complexation of metal ions [15]. Macrocyclic complexes of $Cu(II)$ have been reported to interact with DNA by different binding modes and exhibited efficient nuclease activity [16,17] but unfortunately have received little attention. However, the exact mode and extent of binding and cleavage mechanism still remain unknown leaving behind a scope for an extensive studies involving macrocycles with different structures to evaluate and understand the feature that determine the mode of the binding interaction with DNA and mechanism. The metal complexes of 2'-methylacetoacetanilide and its derivatives have been reported to show interesting biochemical properties such as antitumour, antioxidant, antifungal

* Corresponding author. Tel.: +91 9456033667.

E-mail address: takhan213@yahoo.co.in (T.A. Khan).

¹ Present address: Chemistry Department, College of Science, King Khaled University-Abha, Kingdom of Saudi Arabia.

and antimicrobial activities [18] and laboratory uses and many industrial applications [19]. N. Raman and C. Thangaraju have reported a fully conjugated tetraazamacrocyclic Schiff base ligand by condensation reaction 3'-cinnamalideneacetanilide and o-phenylenediamine and its bivalent metal complexes [20].

Therefore, we thought it worth to synthesize macrocyclic ligands involving 2'-methylacetacetanilide and their complexes and to investigate their spectro-chemical and DNA binding properties. Herein two novel 14- and 16-membered Schiff base tetraaza-macrocyclic ligands are reported by [2+2] condensation reaction of 2'-methylacetacetanilide with 1,2-diaminoethane and 1,3-diaminopropane, respectively and their complexes with Co(II), Ni(II), Cu(II) and Zn(II) ions.

2. Experimental

2.1. Materials and methods

The chemicals, 2'-methylacetacetanilide, 1,2-diaminoethane, 1,3-diaminopropane (Acros, India) were commercially pure compounds and used as such. Metal salts (all Merck) were used as received. Methanol used as a solvent was dried before use [21]. Highly polymerized calf thymus DNA sodium salt (7% Na content) was purchased from Sigma Chemical Co. Other chemicals were of reagent grade and used without further purification. Deionized water was used through out the study. Calf thymus DNA was dissolved to 0.5% w/w, (12.5 mM DNA/phosphate) in 0.1 M sodium phosphate buffer (pH 7.40) at 310 K for 24 h with occasional stirring to ensure formation of homogeneous solution. The purity of the DNA solution was checked from the absorbance ratio A_{260}/A_{280} . Since the absorption ratio lies in the range $1.8 < A_{260}/A_{280} < 1.9$, therefore no further deproteinization of DNA was needed. The stock solution of complexes **1d** and **2d** with 5 mg/ml concentration was also prepared.

2.2. Synthesis of 7,14-dimethyl-5,12-di(N-amino)-2-methylphenyl-1,4,8,11-tetraaza-cyclotetradecane-4,7,11,14-tetraene (L^1)

A solution of 1,2-diaminoethane (0.002 mol, 0.13 ml) taken in 20 cm³ of methanol was slowly added to a methanolic solution (~20 cm³) of 2'-methylacetacetanilide (0.002 mol, 0.382 g) placed in round bottom flask. The reaction mixture was stirred overnight followed by refluxing for 6 h. The reaction mixture was allowed to stand at room temperature resulting in the isolation of microcrystalline solid product after couple of days. The product was washed several times with methanol and dried in vacuo.

2.3. Synthesis of 8,16-dimethyl-6,14-di(N-amino)-2-methylphenyl-1,5,9,13-tetraaza-cyclohexadecane-5,8,13,16-tetraene (L^2)

The same procedure was adopted for the synthesis of L^2 as for L^1 except that 1,3-diaminopropane was used instead of 1,2-diaminoethane.

2.4. Preparation of the complexes, $[ML^1](NO_3)_2$ [$M = Co(II), Ni(II), Cu(II)$ and $Zn(II)$]

To a methanolic solution (~25 cm³) of the hydrated metal nitrate (0.001 mol) taken in round bottom flask was slowly added a methanolic solution (~20 cm³) of ligand, L^1 (0.001 mol, 0.430 gm). The reaction mixture was stirred for 6 h followed by refluxing for 4 h. Microcrystalline solid product was isolated on evaporation over a period of a few days. The product was washed several times with methanol and dried in vacuo.

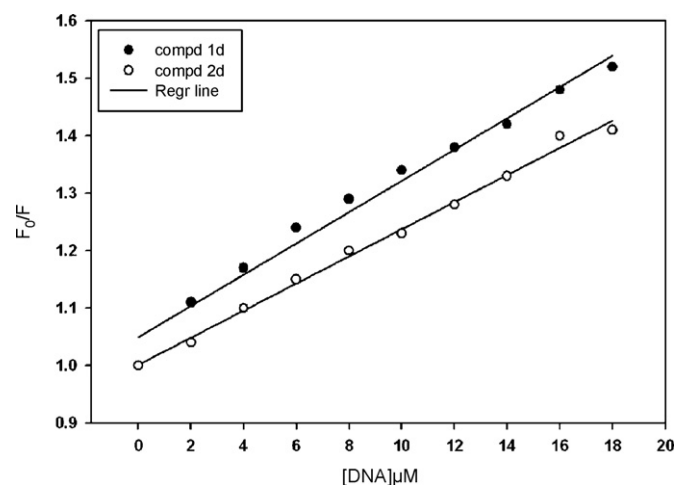


Fig. 1. Stern–Volmer plot for the binding of complexes **1d** and **2d** with DNA at 310 K.

2.5. Preparation of the complexes, $[ML^2](NO_3)_2$ [$M = Co(II), Ni(II), Cu(II)$ and $Zn(II)$]

A similar procedure was adopted for the synthesis of complexes of L^2 (0.001 mol, 0.458 g) as for complexes derived from L^1 .

2.6. Binding analysis of complexes **1d** and **2d**

To elaborate the fluorescence quenching mechanism the Stern–Volmer Eq. (1) was used for data analysis [22]:

$$\frac{F_0}{F} = 1 + K_{sv}[Q] \quad (1)$$

where F_0 and F are the steady-state fluorescence intensities in the absence and presence of quencher, respectively. K_{sv} the Stern–Volmer quenching constant and $[Q]$ is the concentration of quencher (DNA). The K_{sv} for the complex **1d** ($2.7 \times 10^4 \text{ LM}^{-1}$) was found to be onefold higher than the K_{sv} of complex **2d** ($2.4 \times 10^4 \text{ LM}^{-1}$). A higher K_{sv} value of **1d** as compared to **2d** suggests its stronger quenching ability. Further implicates its higher binding affinity toward the DNA than **2d**. The linearity of the F_0/F versus $[Q]$ (Stern–Volmer) plots for DNA–**1d** and **2d** complexes (Fig. 1) depicts that the quenching may be static or dynamic, since the characteristic Stern–Volmer plot of combined quenching (both static and dynamic) is an upward curvature. When ligand molecules

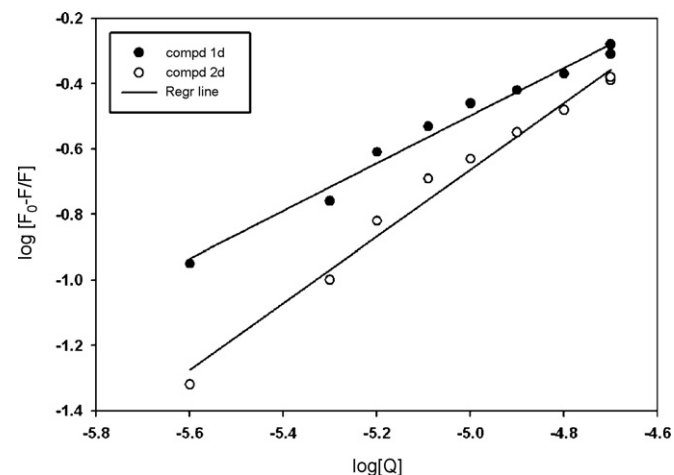


Fig. 2. Comparative plot of $\log((F_0 - F)/F)$ versus $\log[Q]$ for determining the binding constant and number of binding sites, of complexes **1d** and **2d** on DNA.

bind independently to a set of equivalent sites on a macromolecule, the equilibrium between free and bound molecules is given by Eq. (2) [23]:

$$\log \left[\frac{F_0 - F}{F} \right] = \log K + n \log [Q] \quad (2)$$

where K and n are the binding constant and the number of binding sites, respectively. Thus, a plot of $\log (F_0 - F)/F$ versus $\log [Q]$ (Fig. 2), is used to determine K as well as n . The binding parameters for complexes **1d** and **2d** were found to be $K = (27.5 \pm 0.81) \times 10^3 \text{ M}^{-1}$; $n = 1.02$ and $K = (1.39 \pm 0.41) \times 10^3 \text{ M}^{-1}$; $n = 0.72$, respectively. The results suggest that the compound have different degrees of affinity toward the DNA molecule. This differential binding of **1d** and **2d** is attributed in terms of different molecular structures around the Cu(II) ion.

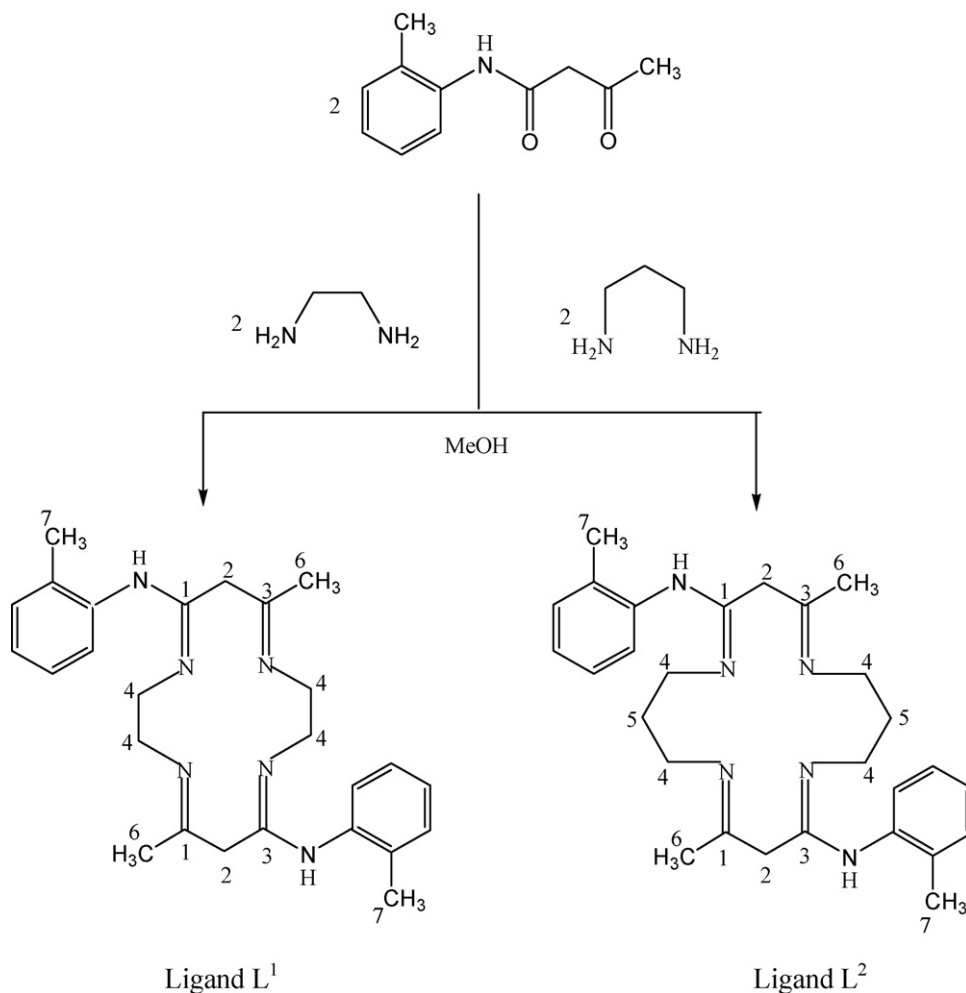
2.7. Physical measurements

The elemental analyses were obtained from the Micro-analytical laboratory of the Central Drug Research Institute (CDRI) Lucknow, India. The IR spectra ($4000\text{--}200 \text{ cm}^{-1}$) were recorded as KBr/CsI discs on the Perkin Elmer–2400 spectrometer. Metal was determined volumetrically [24]. ^1H and ^{13}C -NMR spectra were recorded in DMSO- d_6 using a Bruker Avance II 400 NMR spectrometer with Me_4Si as an internal standard from SAIF, Punjab University, Chandigarh. Electrospray mass spectra of the ligands and its complexes were recorded on a micromass quattro II triple quadrupole mass spectrometer. Magnetic susceptibility measurements were carried

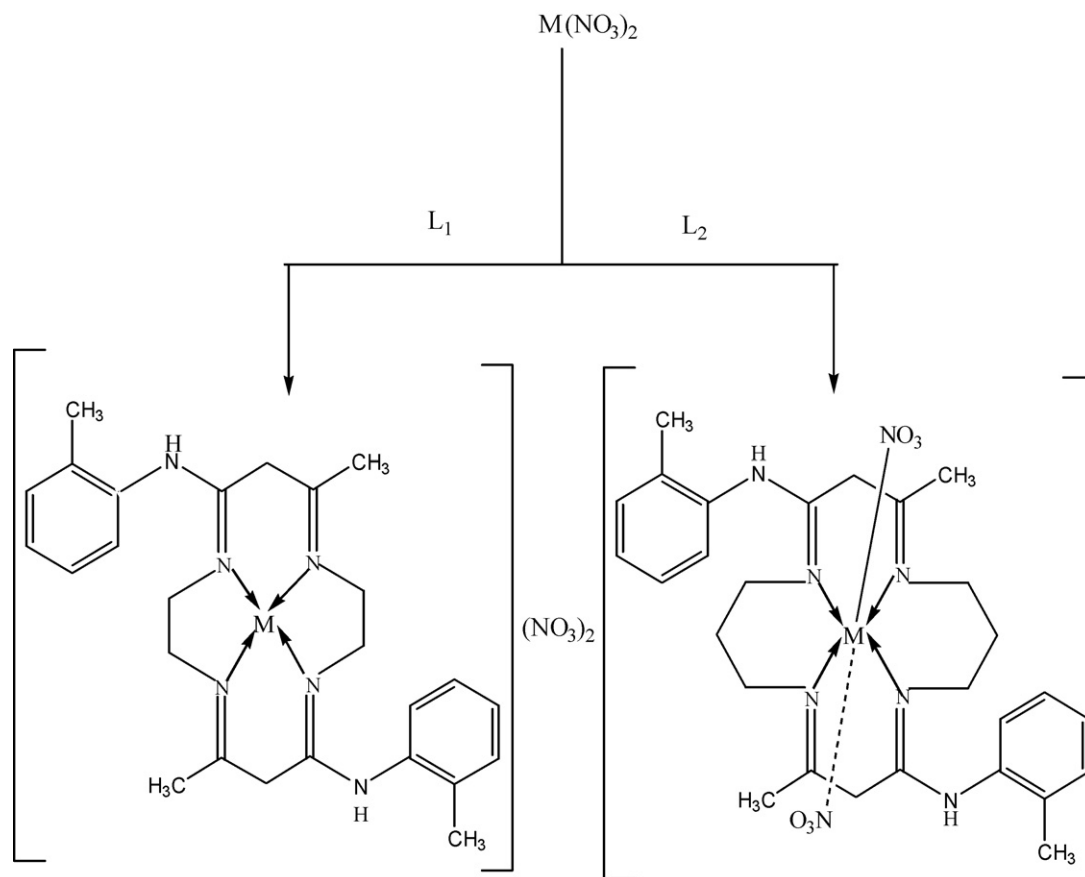
out using a Faraday balance at 25°C . The UV–visible spectrophotometric studies of the freshly prepared 10^{-3} M DMSO solutions of the complexes in the range $200\text{--}1100 \text{ nm}$ were conducted using a Cintra 5 GBC scientific Spectrophotometer at room temperature. EPR spectra were recorded at room temperature on a varian E-4 X-band spectrometer using TCNE as the g-marker. The electrical conductivities (10^{-3} M solution in DMSO) were obtained on a Systronic type 302 conductivity bridge thermostated at $25.00 \pm 0.05^\circ\text{C}$. Fluorescence measurements were performed on a spectrofluorimeter Model RF-5301PC (Shimadzu, Japan) equipped with a 150 W Xenon lamp and a slit width of 3 nm. A 1.00 cm quartz cell was used for measurements. For the determination of binding parameters, $50 \mu\text{M}$ of complex solution was taken in a quartz cell and increasing amounts of ctDNA solution were titrated. Fluorescence spectra were recorded at temperature 310 K in the range of $300\text{--}400 \text{ nm}$ upon excitation at 266 (λ_{em} was 336 nm). The UV measurements of calf thymus DNA were recorded on a Shimadzu double beam spectrophotometer model-UV 1700 using a cuvette of 1 cm path length. Absorbance values of DNA in the absence and presence of complex were made in the range of $225\text{--}290 \text{ nm}$. DNA concentration was fixed at 0.2 mM, while the compound was added in increasing concentrations.

3. Results and discussion

Schiff base macrocyclic ligands were prepared by [2+2] condensation reaction between 2'-methylacetoacetanilide and aliphatic diamines, 1,2-diaminoethane (L^1) or 1,3-diaminopropane



Scheme 1. Formation and Suggested structure of macrocyclic ligands.



Scheme 2. Suggested structure of $[M(L^1)](NO_3)_2$ and $[M(L^2)](NO_3)_2$, where $M = Co(II), Ni(II), Cu(II)$ and $Zn(II)$.

(L^2) (Scheme 1). The complexes of the types, $[ML^1](NO_3)_2$ and $[ML^2](NO_3)_2$ [$M = Co(II), Ni(II), Cu(II)$ and $Zn(II)$] were synthesized by reacting with the ligands, L^1 and L^2 respectively in the presence of appropriate metal nitrate in 1:1 molar ratio

(Scheme 2). The purity of the ligands and the complexes was checked by TLC run in 3:1 chloroform to methanol ratio. The formation of ligand frameworks and the complexes, was deduced on the basis of results of elemental analyses, molecular ion peak

Table 1
Elemental analyses, m/z values, colors, yields, molar conductances, and melting points of the ligands and their complexes.

Complexes	m/z found (calc.)	Color	Yield (%)	M	Found (calc.) (%)		N	Molar conductivity ($\text{ohm}^{-1} \text{cm}^2 \text{mol}^{-1}$)/m.p. ($^{\circ}\text{C}$)
					C	H		
Ligand L^1 1a $C_{26}H_{34}N_6$	430.68 (430.59)	Cream	62	–	72.12 (72.52)	7.46 (7.96)	19.35 (19.52)	–/166
Ligand L^2 2a $C_{28}H_{38}N_6$	458.72 (458.65)	Light yellow	61	–	73.25 (73.33)	8.11 (8.35)	18.20 (18.32)	–/164
$[Co(L^1)](NO_3)_2$ 1b $C_{26}H_{34}CoN_8O_6$	613.59 (613.54)	Brown	70	9.63 (9.61)	50.90 (50.89)	5.60 (5.58)	18.25 (18.26)	120/280
$[Co(L^2)](NO_3)_2$ 2b $C_{28}H_{38}CoN_8O_6$	641.60 (641.59)	Brown	72	9.20 (9.18)	52.39 (52.42)	5.92 (5.97)	17.42 (17.46)	18/246
$[Ni(L^1)](NO_3)_2$ 1c $C_{26}H_{34}NiN_8O_6$	613.34 (613.29)	Blue	71	9.53 (9.57)	50.90 (50.92)	5.60 (5.58)	18.25 (18.27)	110/253
$[Ni(L^2)](NO_3)_2$ 2c $C_{28}H_{38}NiN_8O_6$	641.37 (641.35)	Grey	70	9.20 (9.15)	52.48 (52.44)	5.90 (5.97)	17.50 (17.47)	19/250
$[Cu(L^1)](NO_3)_2$ 1d $C_{26}H_{34}CuN_8O_6$	618.16 (618.15)	Light purple	63	10.22 (10.28)	50.55 (50.52)	5.59 (5.54)	18.10 (18.13)	115/278
$[Cu(L^2)](NO_3)_2$ 2d $C_{28}H_{38}CuN_8O_6$	646.23 (646.19)	Blue	65	9.83 (9.83)	52.10 (52.04)	5.95 (5.93)	17.38 (17.34)	17/264
$[Zn(L^1)](NO_3)_2$ 1e $C_{26}H_{34}ZnN_8O_6$	619.92 (619.98)	Light yellow	68	10.55 (10.55)	50.37 (50.37)	5.50 (5.53)	18.12 (18.07)	112/256
$[Zn(L^2)](NO_3)_2$ 2e $C_{28}H_{38}ZnN_8O_6$	648.18 (648.04)	Light yellow	69	10.10 (10.09)	51.90 (51.89)	5.85 (5.91)	17.25 (17.29)	20/260

Table 2
IR spectral data of the ligands and their complexes (cm⁻¹).

Complexes	$\nu(\text{C}=\text{N})$	$\nu(\text{N}-\text{H})$	$\nu(\text{C}-\text{H})$	$\delta(\text{C}-\text{H})$	$\nu(\text{M}-\text{N})$	$\nu(\text{M}-\text{O})$	Ring Vibration		
Ligand L ¹	1630 s	3250 s	2930 s	1460 s	–	–	1440 s	1060 s	745 s
Ligand L ²	1635 s	3250 s	2925 s	1465 s	–	–	1450 s	1050 s	740 s
[Co(L ¹)](NO ₃) ₂	1600 s	3245 s	2910 s	1450 s	485 m	–	1430 s	1070 s	740 s
[Co(L ²)](NO ₃) ₂	1595 s	3246 s	2915 s	1445 s	490 m	235 m	1420 s	1080 s	745 s
[Ni(L ¹)](NO ₃) ₂	1590 s	3240 s	2925 s	1455 s	480 m	–	1450 s	1080 s	760 s
[Ni(L ²)](NO ₃) ₂	1600 s	3245 s	2930 s	1462 s	485 m	240 m	1430 s	1070 s	750 s
[Cu(L ¹)](NO ₃) ₂	1605 s	3248 s	2885 s	1470 s	495 m	–	1440 s	1030 s	750 s
[Cu(L ²)](NO ₃) ₂	1610 s	3244 s	2880 s	1480 s	500 m	230 m	1460 s	1040 s	735 s
[Zn(L ¹)](NO ₃) ₂	1595 s	3242 s	2920 s	1475 s	500 m	–	1480 s	1040 s	755 s
[Zn(L ²)](NO ₃) ₂	1590 s	3246 s	2915 s	1470 s	495 m	235 m	1470 s	1050 s	750 s

*s = strong; **m = medium.

Table 3
¹H NMR spectra of the ligands and their Zn(II) complexes δ (ppm).

Complexes	–CH ₃ (12H)	N–CH ₂ –C (8H)	C–CH ₂ –C (4H)	NH (2H)	Aromatic (8H)
	δ (s)	δ (t)	δ (m)	δ (s)	δ (m)
L ¹	2.35	2.83	–	8.55	7.67
L ²	2.37	2.88	1.56	8.52	7.72
[Zn(L ¹)](NO ₃) ₂	2.46	2.96	–	8.57	7.80
[Zn(L ²)](NO ₃) ₂	2.57	2.98	1.72	8.56	7.86

Table 4
¹³C NMR spectral data (ppm) of the ligands.

Carbon position	L ¹	L ²
C ₁ and C ₃	158	169
C ₂	85.26	86.12
C ₄	44.26	43.82
C ₅	–	32.82
C ₆	20.12	20.9
C ₇	18.12	18.75
Aromatic carbon	130.1, 137.6, 138.6, 142.5, 141.3	129.0, 135.6, 136.5, 143.7, 142.7

in ESI-mass spectra (Table 1), characteristic bands in the FT-IR (Table 2), and resonance signals in the ¹H and ¹³C NMR spectra (Tables 3 and 4). The overall geometry of the complexes was inferred from the observed values of magnetic moments and the position of bands in the EPR and electronic spectra (Table 5). The molar conductance measurements of all the complexes in DMSO corresponding to ligand L¹ show 1:2 electrolytic nature while complexes of ligand L² exhibit non electrolyte nature.

Table 5
Magnetic moments, electronic spectral bands (cm⁻¹) with their assignments and EPR data of the complexes of L¹ and L² ligands.

Complexes	μ_{eff} (BM)	Band position (cm ⁻¹)	Assignments	EPR Parameters		
				g_{\parallel}	g_{\perp}	G
[Co(L ¹)](NO ₃) ₂	3.12	17,055	⁴ A _{2g} → ⁴ T _{1g} (P)	–	–	–
		14,960	⁴ A _{2g} → ⁴ T _{1g} (F)			
[Co(L ²)](NO ₃) ₂	4.55	19,841	⁴ T _{1g} (F) → ⁴ T _{1g} (P)	–	–	–
		14,750	⁴ T _{1g} (F) → ⁴ A _{2g} (F)			
[Ni(L ¹)](NO ₃) ₂	Diamagnetic	13,720	¹ A _{1g} (D) → ¹ A _{2g} (G)	–	–	–
		21,207	¹ A _{1g} (D) → ¹ B _{2g} (G)			
		25,070	¹ A _{1g} (D) → ¹ E _g (G)			
[Ni(L ²)](NO ₃) ₂	3.14	10,235	³ A _{2g} (F) → ³ T _{2g} (F)	–	–	–
		16,070	³ A _{2g} (F) → ³ T _{1g} (F)			
		24,517	³ A _{2g} (F) → ³ T _{1g} (P)			
[Cu(L ¹)](NO ₃) ₂	1.72	17,827	² B _{1g} → ² A _{1g}	2.1792	2.0882	2.0317
		22,275	² B _{1g} → ² E _g			
[Cu(L ²)](NO ₃) ₂	1.85	16,500	² B _{1g} → ² B _{2g}	2.0916	2.0507	1.8067
		19,127	² B _{1g} → ² E _g			

3.1. Infrared spectra

The IR spectra (4000–200 cm⁻¹) of the ligands and their metal complexes feature absorption bands characteristics of various functional groups of macrocyclic moiety providing information regarding the formation of macrocyclic ligands and their coordination mode in the complexes (Table 2). The i.r. spectra of both the ligands show a new strong intensity bands at 1630 and 1635 cm⁻¹, which may reasonably be assigned [25] to the imine function $\nu(\text{C}=\text{N})$ in the macrocyclic system. However, no band has been observed characteristic of either free primary amine or carbonyl functions supportive of the formation of proposed macrocyclic skeleton. A significant negative shift (25–40 cm⁻¹) in $\nu(\text{C}=\text{N})$ stretching mode has been observed for the complexes as compared to free ligands suggesting [26] the involvement of imine nitrogen of the (C=N) group in coordination with metal ions. This is further supported by the appearance of a new medium intensity band in the region 480–500 cm⁻¹ assignable [27] to $\nu(\text{M}-\text{N})$ vibration. A broad strong intensity band in the i.r. spectra of ligands and its complexes in the region (3240–3250 cm⁻¹) may reasonably be assigned to secondary amine group. A weak absorption band in the

region 2920–2925 cm⁻¹ may be assigned [28] to CH₃ stretching vibration. All the complexes show sharp bands corresponding to $\nu(\text{C-H})$, $\delta(\text{C-H})$ and phenyl ring vibrations which appear at their expected positions (Table 2). The coordination of nitrate groups has been ascertained by appearance of bands in 230–240 cm⁻¹ regions, which may reasonably be assigned [29] to $\nu(\text{M-O})$ of the O-NO₂ group in [M(L²)(NO₃)₂] complexes. The IR spectra of these complexes show further bands in 1230–1270, 1040–1070 and 860–890 cm⁻¹ region, which are consistent with monodentate coordination of the nitrate group [29]. However, the bands corresponding to free nitrate group in [ML¹](NO₃)₂ complexes appear in the region 1384–1390 cm⁻¹ [30].

3.2. ¹H NMR spectra

The ¹H NMR data for macrocyclic ligands and their Zn(II) complexes (Table 3) recorded in DMSO-*d*₆ show a sharp signal in the region δ 2.35–2.57 which may be assigned to the methyl protons (-CH₃; 12H). However, a singlet at \sim δ 8.55 may be attributed to the pendant secondary amino protons (C-NH-C; 2H) [20]. A triplet observed in the region δ 2.83– δ 2.88 for L¹ and L² corresponds [31] to the methylene protons (N-CH₂-C; 8H) adjacent to the nitrogen atom of the imine function of macrocyclic framework. Another multiplet at δ 1.56 may reasonably be assigned [31] to the middle methylene protons (C-CH₂-C; 4H) of the 1,3-diaminopropane moiety in ligand L². A multiplet observed in the range δ 7.67– δ 7.72 for L¹ and L² may be attributed to the phenyl protons (C₆H₄; 8H) [20]. However, the resonance signals obtained for Zn(II) complexes show downfield shift as compared to the corresponding ligands (Table 3) indicating the coordination of ligands to Zn(II) ion.

3.3. ¹³C NMR

The ¹³C NMR spectra of the ligands and their Zn(II) complexes recorded in DMSO-*d*₆ at room temperature gave ¹³C NMR signals characteristic of carbon atoms of imine functions and all other carbons in the macrocyclic skeleton at their appropriate positions corresponding to the proposed structure. However, the position of peaks in complexes compared with the free Schiff base macrocyclic ligands (Table 4) show slight shifts invoking coordination of the ligands to Zn(II) ion [20].

3.4. EPR spectra

The EPR spectra of Cu(II) complexes were recorded as polycrystalline sample on X-Band at frequency 9.1 GHz under the magnetic field strength 3100 G scan rate 1000, recorded at room temperature (Fig. 3a and b). The g_{\parallel} , g_{\perp} and G values obtained from these spectra are presented in Table 5. The g_{\parallel} and g_{\perp} values were computed from the spectrum using TCNE free radical as 'g' marker. In square planar and distorted octahedral geometry, the unpaired electron lies in the $d_{x^2 - d_{y^2}}$ orbital giving ²B_{1g} as the ground state with $g_{\parallel} > g_{\perp}$. The observed g values (Table 5) are characteristic of a square planar and a distorted octahedral geometry in complexes [Cu(L¹)](NO₃)₂ and [Cu(L²)(NO₃)₂], respectively. Kivelson and Neiman [32] have reported the $g_{\parallel} < 2.3$ for covalent character of the metal ligand bond and $g_{\parallel} > 2.3$ for ionic character. Applying this criterion the covalent character of the metal ligand bond in the complexes under study can be predicted. The trend $g_{\parallel} > g_{\perp} > g_e$ (2.0023) observed for these complexes show that the unpaired electron is localized in $d_{x^2 - d_{y^2}}$ orbital of the Cu(II) ions. The g values are related by the expression

$$G = \frac{g_{\parallel} - 2}{g_{\perp} - 2}$$

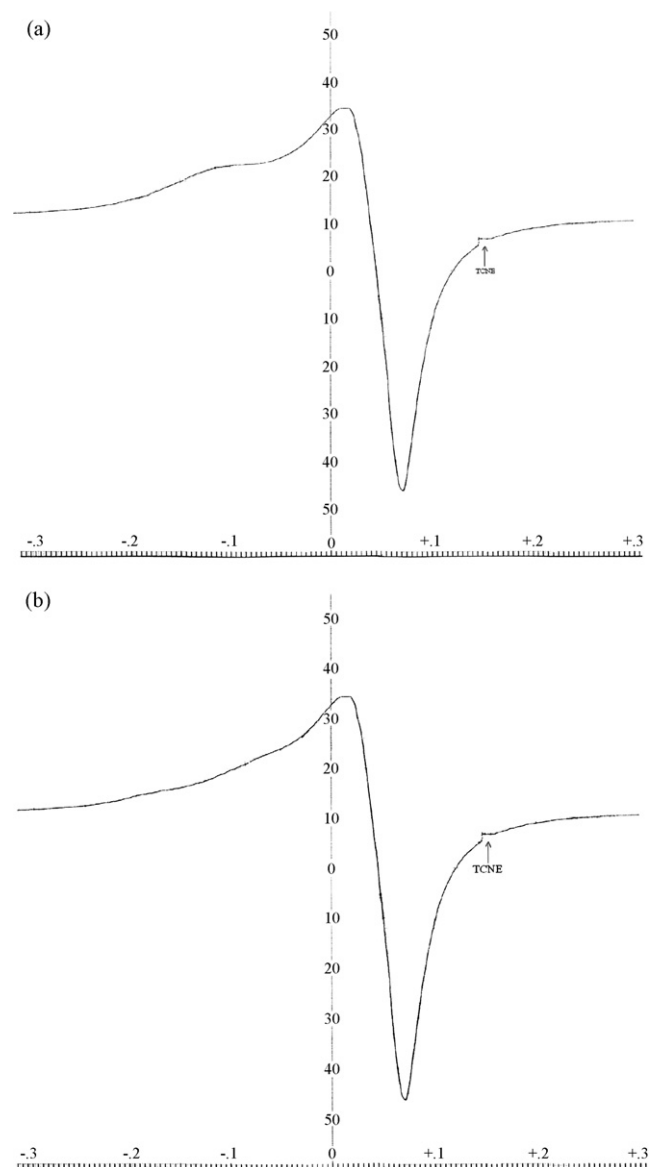


Fig. 3. (a) EPR spectra of the complex **1d** at room temperature. (b) EPR spectra of the complex **2d** at room temperature.

which measure the exchange interaction between the copper centers in the polycrystalline solid. If $G > 4$, the exchange interaction is negligible and if $G < 4$ considerable exchange interaction occurs in solid complexes [33]. The G values in the range 1.8067–2.0317, indicate for these complexes considerable interaction between two copper centers.

3.5. Electronic spectra and magnetic moments

The electronic spectra of the complexes were recorded in DMSO (Table 5). The electronic spectrum of [Co(L¹)](NO₃)₂ shows two absorption bands at 17,055 and 14,960 cm⁻¹ assignable to ⁴A_{2g} → ⁴T_{1g}(P) and ⁴A_{2g} → ⁴T_{1g}(F) transitions, respectively and a band at 22,730 cm⁻¹ assignable to $\pi \rightarrow \pi^*$ transition. These transition are in support of a square-planar geometry [20]. This is further supported by observed magnetic moment of 3.12 B.M. The observed magnetic moment of 4.55 B.M. and absorption bands in the electronic spectrum at 14,750 and 19,841 cm⁻¹ assigned to the ⁴T_{1g}(F) → ⁴A_{2g}(F) and ⁴T_{1g}(F) → ⁴T_{1g}(P) transitions, respectively for the [Co(L²)(NO₃)₂] are consistent with an octahedral environment

around the Co(II) ion in the complex similar to that reported earlier [34].

The electronic spectrum of $[\text{Ni}(\text{L}^1)](\text{NO}_3)_2$ exhibits three absorption bands at 13,720, 21,207 and 25,070 cm^{-1} which may be assigned to the three spin allowed transitions, $^1\text{A}_{1\text{g}}(\text{D}) \rightarrow ^1\text{A}_{2\text{g}}(\text{G})$, $^1\text{A}_{1\text{g}}(\text{D}) \rightarrow ^1\text{B}_{2\text{g}}(\text{G})$ and $^1\text{A}_{1\text{g}}(\text{D}) \rightarrow ^1\text{E}_{\text{g}}(\text{G})$, respectively characteristic of square planar geometry around Ni(II) ion [31]. The diamagnetic nature revealed by magnetic moment studies further confirm the square planar environment around the Ni(II) ion [31]. While the observed magnetic moment value of 3.14 B.M. of $[\text{Ni}(\text{L}^2)](\text{NO}_3)_2$ and three electronic spectral bands at 10,235, 16,070 and 24,517 cm^{-1} corresponding to three spin allowed transitions $^3\text{A}_{2\text{g}}(\text{F}) \rightarrow ^3\text{T}_{2\text{g}}(\text{F})$, $^3\text{A}_{2\text{g}}(\text{F}) \rightarrow ^3\text{T}_{1\text{g}}(\text{F})$ and $^3\text{A}_{2\text{g}}(\text{F}) \rightarrow ^3\text{T}_{1\text{g}}(\text{P})$, respectively indicate an octahedral geometry [35].

The spectrum of $[\text{Cu}(\text{L}^1)](\text{NO}_3)_2$ shows two bands in the visible region, at 17,827 and 22,275 cm^{-1} assignable to $^2\text{B}_{1\text{g}} \rightarrow ^2\text{A}_{1\text{g}}$ and $^2\text{B}_{1\text{g}} \rightarrow ^2\text{E}_{\text{g}}$ transitions, respectively and the observed magnetic moment of the complex is 1.72 B.M. similar to the square planar complexes of Cu(II) ion [20].

The electronic spectra of $[\text{Cu}(\text{L}^2)](\text{NO}_3)_2$ show a shoulder at 16,500 cm^{-1} with a main broad band at 19,127 cm^{-1} which may unambiguously be assigned to $^2\text{B}_{1\text{g}} \rightarrow ^2\text{B}_{2\text{g}}$ and $^2\text{B}_{1\text{g}} \rightarrow ^2\text{E}_{\text{g}}$ transitions, respectively consistent with those reported for a distorted octahedral geometry [35] around the Cu(II) ion. The observed magnetic moments of 1.85 B.M. further complement the electronic spectral results [35].

3.6. Fluorescence measurements

3.6.1. Binding property of the DNA to complexes **1d** and **2d**

The fluorescence spectroscopy provides insight of the changes taken place in the microenvironment of DNA molecule on ligand binding. The binding of these compounds with calf thymus DNA, were studied by monitoring the changes in the intrinsic fluorescence of these compounds at varying DNA concentration. Fig. 4a and b, show the representative fluorescence emission spectra of the synthesized compound upon excitation at 266 nm. The addition of DNA caused a gradual decrease in the fluorescence emission intensity of both the compounds with a conspicuous change in the emission spectra. The spectra illustrate that an excess of DNA led to more effective quenching of the fluorophore molecule fluorescence. The quenching of the compound fluorescence clearly indicated that the binding of the DNA to complexes **1d** and **2d** changed the microenvironment of fluorophore residue. The shift in emission peak of the synthesized molecule further depicts effective interaction at higher DNA concentration, which is more prominent in case of **1d**. The reduction in the intrinsic fluorescence of synthesized molecules upon interaction with DNA could be due to masking or burial of compound fluorophore upon interaction between the stacked bases with in the helix and/or surface binding at the reactive nucleophilic sites on the heterocyclic nitrogenous bases of DNA molecule.

3.7. Absorption spectroscopy

UV–Vis absorption studies were performed to further ascertain the DNA-complexes **1d** and **2d** interaction. The UV absorbance showed an increase with the increase in the complex **1d/2d** concentrations (Fig. 5). Since the complexes **1d** and **2d** do not show any peak in this region (Fig. 5), hence the rise in the DNA absorbance is indicative of the interaction between DNA and the complexes **1d/2d** molecules. Both complexes exhibited hyperchromism but of varied degree. Slight bathochromic shift was observed with complex **1d**, which was negligible with complex **2d**. As hypochromism and hyperchromism are both the spectral features of DNA concerning of its double helix structure. Hypochromism means the DNA binding

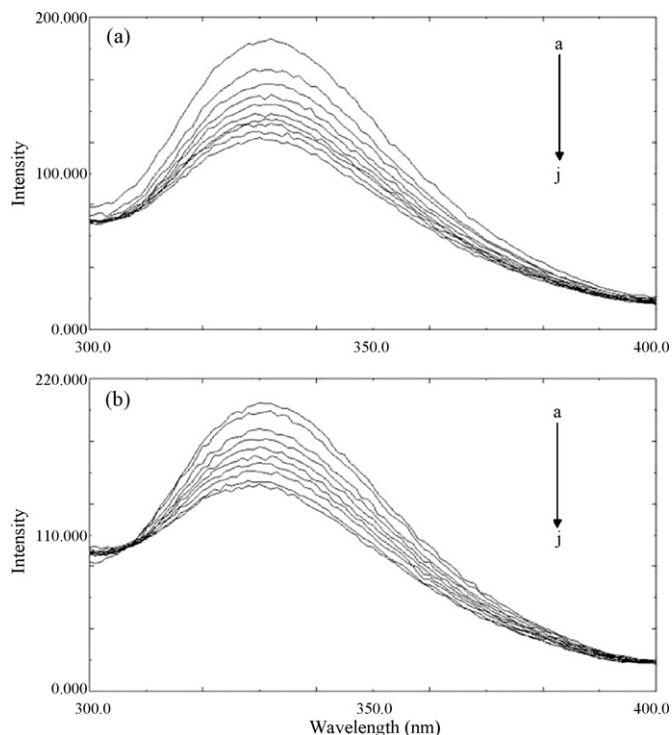


Fig. 4. Fluorescence emission spectra of complexes **1d** (a) and **2d** (b) in the absence and presence of increasing amount of DNA (a) 0 (b) 5 (c) 10 (d) 15 (e) 20 (f) 25 (g) 30 (h) 35 (i) 40 and (j) 45 μM ; pH 7.4; $T = 298\text{K}$.

mode of complex is electrostatic effect or intercalation which can stabilize the DNA duplex [36,37], and hyperchromism means the breakage of the secondary structure of DNA. So we primarily speculate that the complex interacting with the secondary structure

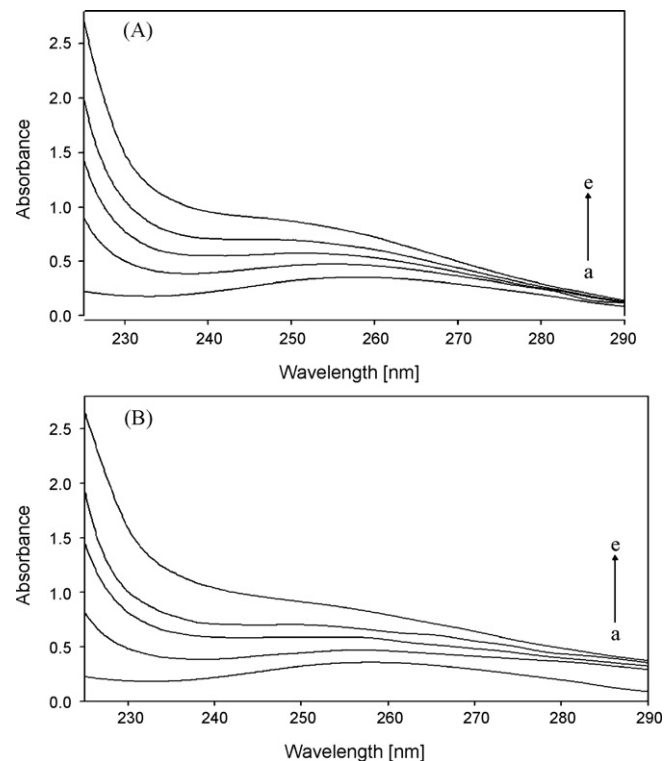


Fig. 5. Absorbance spectra of DNA and DNA-**1d** (A)/**2d** (B) system. DNA concentration was 0.20 mM (a). **1d/2d** concentration for DNA-compound system was at 12.5 μM (b), 25 μM (c), 50 μM (d) and 100 μM (e).

with calf thymus DNA resulting in its breakage and perturbation. After interaction with the base pairs of DNA, the π – π^* orbital of the bound ligand can couple with the π orbital of the base pairs, due to the decrease π – π^* transition energy, which results in bathochromic shift [38]. The shift in the spectra of **1d** suggests the more interference of orbital by this molecule, which also corroborates with the high binding affinity of this **1d**. The above changes are indicative of the conformational alteration of DNA on but of varied extent.

4. Conclusion

The novel 14 and 16 membered Schiff base macrocyclic ligands (L^1) and (L^2) have been synthesized by condensation reaction between 2'-methylacetanilide and aliphatic diamines and their macrocyclic complexes, prepared by interaction of ligands, L^1 or L^2 with hydrated metal(II) nitrates have been characterized by various physico-chemical studies. The ligand to metal stoichiometry and the nature of bonding was ascertained on the basis elemental analyses, position of molecular ion peaks in the mass spectra and conductivity data. The formation of the proposed macrocyclic framework has been inferred by the appearance of imine bands in the IR and corresponding proton resonance signals in the ^1H and ^{13}C NMR spectra. A square planar geometry was deduced for complexes derived from ligand L^1 while an octahedral geometry with slight distortion in $[\text{Cu}(L^2)(\text{NO}_3)_2]$ complex was inferred for complexes resulted from Ligand L^2 on the basis of UV–visible and EPR spectral studies and magnetic moment data. The fluorescence and absorption studies demonstrated a considerable interaction between the complexes **1d** and **2d** and calf thymus DNA.

Acknowledgments

The Chairman, Department of Chemistry, Aligarh Muslim University, Aligarh, India is acknowledged for providing the necessary research facilities. The authors thank the Regional Sophisticated Instrumentation Center, CDRI Lucknow for providing mass spectral and analytical data for the compounds.

References

- [1] W. Radecka-Paryzek, V. Patroniak, J. Lisowski, *Coord. Chem. Rev.* 249 (2005) 2156.

- [2] S. Chandra, X. Sangeetika, *Spectrochim. Acta* 60 A (2004) 147.
 [3] Min Wang, Liu-Fang Wang, Yi-Zhi Li, Qin-Xi-Li, Zhi-Dong Xu, Dong-Ming Qu, *Trans. Met. Chem.* 26 (2001) 307.
 [4] N.N. Gulerman, S. Rollas, H. Erdeniz, M. Kiraj, *J. Pharm. Sci.* 26 (11) (2001) 1.
 [5] V. Mishra, S.N. Pandeya, S. Anathan, *Acta Pharmaceutica Turcica* 42 (4) (2000) 139.
 [6] P. Tarasconi, S. Capacchi, G. Pelosi, M. Cornia, R. Albertini, A. Bonati, P.P. Dall'Aglio, P. Lunghi, S. Pinelli, *Bioorganic. Med. Chem.* 8 (2000) 154.
 [7] S. Chandra, K. Gupta, *Trans. Met. Chem.* 27 (2002) 196.
 [8] L. Valencia, H. Adams, R. Bastida, D.E. Fenton, A. Macias, *Inorg. Chim. Acta* 317 (2001) 45.
 [9] A.A. Saleh, *J. Coord. Chem.* 58 (3) (2005) 255.
 [10] D.S. Kumar, V. Alexander, *Polyhedron* 18 (1999) 1561.
 [11] J.L. Sessler, R.A. Miller, *Biochem. Pharmacol.* 59 (2000) 733.
 [12] A. Martell, J. Penitka, D. Kong, *Coord. Chem. Rev.* 216 (2001) 55.
 [13] (a) V. McKee, in: A.G. Sikes (Ed.), *Advanced in Inorganic Chemistry*, vol. 40, Academic Press, San Diego, USA, 1993, p. 323;
 (b) S. Brooker, *Coord. Chem. Rev.* 222 (2001) 33.
 [14] H. Keypour, H. Goudaziafshar, A.K. Brisdon, R.G. Pritchard, M. Rezaeivala, *Inorg. Chim. Acta* 361 (2008) 1415.
 [15] A. Golcu, M. Tumer, H. Demirelli, R.A. Wheatley, *Inorg. Chim. Acta* 358 (2005) 1785.
 [16] C.-L. Liu, J.-Y. Zhou, Q.-X. Li, L.-J. Wang, Z.-R. Liao, H.-B. Xu, *J. Inorg. Biochem.* 75 (1999) 233.
 [17] D.K. Chand, H.J. Schneider, J.A. Aguilar, F. Escarti, E. Garcia-Esspara, S.V. Luis, *Inorg. Chim. Acta* 316 (2001) 71.
 [18] K. Krishnankutty, M.B. Ummathur, *J. Indian Chem. Soc.* 83 (2006) 883.
 [19] R.E. Sievers, S.B. Turnispeed, L. Huang, A.F. Laglante, *Coord. Chem. Rev.* 128 (1993) 285.
 [20] N. Raman, C. Thangaraja, *Trans. Met. Chem.* 30 (2005) 317.
 [21] A.I. Vogel, *A Text Book of Quantitative Inorganic Analysis*, third ed., Longmans, London, 1961.
 [22] A.M. Pyle, J.P. Rehmann, R. Meshoryer, C.V. Kumar, N.J. Turro, J.K. Barton, *J. Am. Chem. Soc.* 111 (1989) 3051.
 [23] X.-Z. Feng, Z. Lin, L.-J. Yang, C. Wang, C.-L. Bai, *Talanta* 47 (1998) 1223.
 [24] C.N. Reilly, R.W. Schmid, F.S. Sadek, *J. Chem. Ed.* 36 (1959) 619.
 [25] N. Nishat, Rahis-ud-din, M.M. Haq, *Trans. Met. Chem.* 28 (2003) 948.
 [26] P.R. Athapan, G. Rajagopal, *Polyhedron* 15 (1990) 527.
 [27] M. Shakir, N. Begum, S. Parveen, P. Chingsubam, S. Tabassum, *Synth. React. Inorg. Met.-Org. Chem.* 34 (2004) 1135.
 [28] N. Raman, *J. Indian Chem. Soc.* 84 (2007) 29.
 [29] M. Shakir, Y. Azim, H.T.N. Chishti, N. Begum, P. Chingsubam, M.Y. Siddiqi, *J. Braz. Chem. Soc.* 17 (2006) 272.
 [30] K. Nakamoto, *Infrared and Raman Spectra of Inorganic and Coordination Compounds*, Wiley/Interscience, New York, NY, 1970.
 [31] S. Chandra, L.K. Gupta, D. Jain, *Spectrochim. Acta* 60 A (2004) 2411.
 [32] D. Kivelson, R. Neiman, *J. Chem. Phys.* 35 (1962) 149.
 [33] B.J. Hathaway, in: J.N. Bradley, R.D. Gillard (Eds.), *Essays in Chemistry*, Academic Press, New York, 1971.
 [34] A.B.P. Liver, *Inorganic Electronic Spectroscopy*, second ed., Elsevier, Amsterdam, 1984.
 [35] F.A. Cotton, G. Wilkinson, *Advanced Inorganic Chemistry*, fifth ed., John Wiley, Singapore, 1988.
 [36] P. Yang, M.-L. Guo, B.-S. Yang, *Chin. Sci. Bull.* 39 (1994) 997.
 [37] E.C. Long, J.K. Barton, *Acc. Chem. Res.* 23 (1990) 271.
 [38] X.F. He, H. Chen, L. Xu, L.N. Ji, *Polyhedron* 17 (1998) 3161.